Coherent control and generation of tunable narrowband terahertz radiation from air-plasma filament driven by two-color pulse sequence

Xiaoyue Zhou[1],[*] Yuchen Lin[1],[*] Fu Deng[1], and Jingdi Zhang[1,2][†]

[1]*Department of Physics, The Hong Kong University of Science and Technology, Kowloon, Hong Kong SAR, China*

[2]*William Mong Institute of Nano Science and Technology, The Hong Kong University of Science and Technology, Kowloon, Hong Kong SAR, China*

Abstract

We report the proof-of-principle experiment of generating carrier-envelope phase (CEP)-controllable and frequency-tunable narrowband terahertz (THz) radiation from air-plasma filament driven by the beat of temporally stretched two-color laser pulse sequence. The pulse sequence was prepared by propagating the fundamental ultrafast laser pulse through a grating stretcher and Michelson interferometer with variable inter-arm delay. It was then partially frequency-doubled and focused to create a two-color field driven air-plasma filament as the source of THz radiation, of which both the center frequency and the CEP can be coherently tuned and controlled. To reproduce experimental results and elucidate complex nonlinear light-matter interaction, numerical simulation has been performed. This work demonstrates the feasibility of generating coherently controlled narrowband THz wave with high tunability in laser-induced air plasma.

[*] The authors contributed equally to this work

[†] Corresponding author email: jdzhang@ust.hk

1

Optical generation and detection of THz radiation have been of increasing interest in the last two decades, owing to its wide range of applications in non-invasive imaging, chemistry, material science [1] and condensed matter physics [2, 3]. THz radiation can be generated from transient current in photoconductive switches, optical rectification in non-linear crystals and wave-mixing in laser-induced two-color air plasma [4]. On the one hand, the two-color laser-induced air-plasma THz source has recently been studied extensively due to its simultaneous delivery of ultrashort pulse duration and ultrabroad spectral range spanning far- and mid-infrared frequencies, which are highly beneficial for advanced ultrafast spectroscopy providing details at an unprecedentedly level [5–9]. On the other hand, table-top narrowband THz source has become highly desirable in order to meet the rapidly growing demands in dynamic investigation and coherent manipulation of novel states in quantum materials, e.g., Floquet engineering [10] and mode-selective excitation [11, 12]. Many efforts have been put into the coherent generation of narrowband THz radiation but mainly rely on light-interaction in solid materials, i.e., photo-conductive antenna [13], lithium niobate crystal (LNO) [14, 15] and organic compounds [16]. However, few attempts have been made to generate tunable narrowband THz wave from gaseous medium, e.g., laser-induced air plasma [17].

As a common problem faced by narrowband THz and mid-infrared generation via non-linear wave-mixing process, long-term CEP walk-off may result from environmental factors leading to either thermal or mechanical drift [18, 19]. Although there exist many representative studies on coherent polarization control on THz radiation from two-color laser air plasma [20–24], generation of narrowband THz with coherently tunable carrier-envelope phase has remained under-explored, a feature highly desired for active CEP stabilization of THz radiation as well as providing new grounds for resonance and phase-sensitive coherent control of novel states of quantum materials [25, 26].

In this letter, we demonstrate the proof-of-principle experiment for the generation of narrowband THz radiation with both frequency and CEP tunability from an air-plasma filament coherently driven by a two-color pulse sequence, generated by the chirped-pulse beating method, a pulse-shaping technique extensively used in table-top [14, 27, 28] and accelerator-based [29, 30] generation of tunable narrowband THz radiation in solid materials and relativistic free-electron bunches, respectively. By adopting this approach, a tunable low-frequency intensity modulation can be imprinted to the stretched Gaussian intensity

profile, of which the duration can continuously vary in accordance with the change in linear chirp of the carrier wave, i.e., second order dispersion [13, 31]. Here, considering an optical pulse with a central frequency of ω_0 and a linear chirp rate β acquired by traversing a stretcher grating, its instantaneous frequency can be expressed as $\omega(t) = \omega_0 + \beta t$. The chirped pulse is subsequently split into halves upon entry of the Michelson interferometer so as to create two replicas at a time delay τ that is tunable by controlling the interfering optical paths. Instantaneous frequencies of individual replicas follow $\omega_1(t) = \omega_0 + \beta(t - \tau)$ and $\omega_2(t) = \omega_0 + \beta t$, respectively. Therefore, a constant differential frequency, i.e., beat note, $\Delta\omega = \beta\tau$ emerges and modulates the intensity profile of the total electric field, that is, superposition of waveform of the two pulsed replicas at delay τ. Such inter-pulse delay τ dependence, in turn, provides us convenient access to controlling the modulation frequency $\Delta\omega$. When combined with the strong-field-induced air-plasma filamentation process, it is the interferometry-based pulsed shaping configuration that gives rise to a pulse sequence, imposing a background periodic modulation to both the violent ionization of air molecules and coherent motion of the resultant free electrons, favorable for coherent enhancement of the quasi-monochromatic emission at the modulation frequency $\Delta\omega$.

The schematic diagram of our experiment is illustrated in Fig. 1. We took the output of a 1 kHz Ti:sapphire amplifier laser system emitting near-IR optical pulses (800 nm in center wavelength, 2 mJ in energy and 100fs in duration). The chirp level could be readily introduced by translating the pulse stretcher comprising a pair of diffraction gratings. To effectively generate narrowband THz radiation, the pulse duration was stretched to 1.2 ps corresponding to a chirp level parameter $C = z\beta_2/T_0^2 = 12$. A Michelson interferometer split the stretched optical pulse into two identical pulses with relative delay τ, the parameter tunable by altering the length of one arm. Upon recombining two beams with a second beam splitter at the interferometer exit port, a pulse sequence with a quasi-sinusoidal modulation of frequency $\Delta\omega$ could be formed and served as the fundamental wave (FW) for subsequent second harmonic generation (SHG) in a BBO crystal. By focusing the two-color laser field, the air-plasma filament appeared and centered slightly before the geometrical focus of the lens due to the self-focusing effect. Considering the long temporal duration of the stretched pulse, the ramification of group velocity mismatch in the BBO crystal, which limits the usable crystal thickness and is commonly suffered by SHG with short pulses, can be significantly reduced. In our experiment, a 500 μm thick BBO crystal was used for optimal second

3

harmonic generation (SHG) efficiency that scales quadratically with the nonlinear crystal thickness. A pair of off-axis parabolic mirrors was placed after the radiation source to collect the generated THz radiation. To filter out higher-frequency components, a silicon wafer (not shown in the figure) was used. Finally, the time-domain waveform of THz radiation was read out by electro-optic sampling (EOS) in ZnTe detection crystal. To minimize the undersampling effect, a transform-limited pulse (100 fs) was used as the gate beam to read out the THz waveform. The entire setup was constantly purged with dry air for elimination of the ambient water vapor absorption.

After stretching the fundamental 100 fs pulse to 1.2 ps, we performed a series of measurements on the time-domain THz signal at various inter-pulse delay τ set by interferometer (Fig. 2). In contrast to the temporal profile of a typical broadband THz signal generated by uncontrolled two-color laser pulse, the generated THz signal by pulse sequence exhibits multi-cycle oscillating characteristics in the time domain, signifying a pronounced reduction in bandwidth. The linear relation of the center frequency of the narrowband THz with respect to delay τ is best demonstrated in the range of 300 to 600 fs. By increasing the delay τ, the center frequency is continuously tuned from 1.28 to 2.02 THz, with the bandwidth becoming the narrowest (0.725 THz) at $\tau = 500$ fs. In order to optimize the output power of the narrowband THz, the spatial overlap between the twin pulses was aligned to be perfectly collinear, and the BBO crystal was oriented to achieve a FW-to-SHG power ratio optimal for THz generation. However, in this scheme, it is not unexpected to observe the limited tuning range in frequency and deformed waveform for narrowband THz generation, particularly when τ is large, that result from two adverse effects, one being the strong phonon absorption in detection crystal and the other being compromised ionization efficiency in a filament under the drive of a stretched laser pulse with a lowered peak intensity.

To supplement the experiment, we perform numerical simulations to gain insight into the microscopic dynamics of the observed phenomena. According to the photocurrent model [32], the superimposed two-color laser field effectively provides an asymmetric field, triggering the tunneling ionization of electrons in the nitrogen atoms, and prescribing a net drift momentum of resultant free electrons. The pertinent quasi-DC motion of free electrons takes place at sub-picosecond timescale and, therefore, radiates at THz frequencies. This process is predictable by Ammosov-Delone-Krainov (ADK) tunneling ionization model [33]

and can be best described by the expression:

$$dJ(t) = \frac{e^2}{m_e}dN \int_0^t (E_\omega^{total} + E_{2\omega}^{total})dt, \tag{1}$$

where e is the elementary charge of electron, m_e is the mass of free electron, dN is the number of ionized electrons in time interval $[t, t+dt]$. The total current density at a given instant t can be expressed as an integration of dJ at all prior instants: $J(t) = \int_{-\infty}^t dJ(t')$. The THz radiation E_{THz} can be related to the electron current density J by $E_{\text{THz}} \propto dJ/dt$. In our experiment, the chirped-and-delayed laser field follows the form $E_\omega^{total} = E_\omega(t) + E_\omega(t+\tau)$, where $E_\omega(t)$ and $E_\omega(t+\tau)$ denote the electric field of the chirped fundamental wave and its delayed replica, respectively. Note that the envelope of E_ω^{total} carries a beat note oscillating at a much lower frequency of $\Delta\omega$ than that of fundamental wave ω. From the equation above, it follows that the concomitant ionization and radiating process repeat at a constant time interval defined by the inverse of beat note. This periodic modulation to the picosecond ionization event is in equivalence to a "multiple-slit" interference in the time domain. As a result, a quasi-monochromatic electromagnetic wave at frequencies in accordance with the beat note can be emitted and detected in the far-field measurement. Fig. 2 (c)(d) show simulation results of time-domain signals of the THz radiation and the corresponding magnitude spectra, respectively, which are in excellent agreement with experimental results. From the figure, central frequencies f_C of measured THz signals for different delay τ agree well with simulations when $f_C < 2$ THz, whereas discrepancies emerge in case $f_C > 2$ THz, an expected trend when considering the above-mentioned limitations.

To demonstrate coherent control over CEP of narrowband THz pulse, a pair of BK7 wedges was inserted into one of the arms of the Michelson interferometer to introduce a relative CEP phase difference $(\Delta\phi)$ between the two stretched near-IR fundamental waves, which collectively displaces nodal points of the beat note underneath the global intensity profile of the pulse sequence. As illustrated in Fig. 3(a), the relative offset between the hump peak and the center of the pulse sequence can be controlled by varying the effective thickness of the wedge pair. This effective phase sliding on pulse sequence translates the timing for periodic modulation of ionization and oscillation of free electrons, which has a one-to-one correspondence to the CEP of the resultant narrowband THz radiation. As indicated by simulation in Fig. 3 (c), a variable inter-pulse CEP difference $\Delta\phi$ to the driving field can coherently control the CEP of narrowband THz radiation. This is, indeed, verified by our

experimental results in Fig. 3 (b). As displacing the wedge pair in transverse direction, we show CEP of the narrowband THz radiation is shifted by $\pi/2$ and π, in agreement with the numerical results.

Our results reported herein admittedly have discrepancies to a certain extent when comparing the theoretical prediction and the experimental results, manifested by non-negligible deformation in the waveform of the time-domain signal and the limited peak field amplitude. In the ideal case, a much wider tuning range and narrower bandwidth of the THz radiation should be feasible upon further improvement of the apparatus. Nevertheless, our experiment demonstrates a new method of generation CEP-controllable and central-frequency-tunable narrowband THz radiation by exploiting Michelson interferometer for coherent control of zero- and first-order inter-pulse phase difference. As a guide to future experiments, we expect increasing the power of the driving pulse sequence and applying DC bias for the facilitation of air-plasma filamentation can significantly improve the THz emission characteristics. We believe these improvements would produce intense narrowband THz radiation, which can serve as an ideal multi-cycle excitation beam in coherent manipulation of quantum materials at THz frequencies. The successful demonstration of the CEP control of the narrowband THz radiation establishes a direct mapping from the CEP of the input optical pulse to the output THz signal exists, implying a potential solution to CEP stabilization of the narrowband THz radiation. Conversely, the detection of the narrowband THz time-domain signal can also be used to probe the phase of the input optical pulse, furnishing a new CEP metrology.

In conclusion, by adopting the chirped-beating method, we have realized the generation of tunable narrowband THz radiation from air plasma induced by two-color laser pulse sequence. Most importantly, the coherent CEP control over the generated narrowband THz radiation has been successfully demonstrated. It was achieved by tuning the zero-order phase difference of the twin pulses used for the synthesis of the periodically modulated pulse sequence, which in turn affects the timing of modulation to the ionized electrons. Our work verified the feasibility of applying the chirped-beating method to two-color laser-induced air plasma scheme and paved the way for the coherent manipulation of narrowband THz radiation characteristics.

---

[1] M. Tonouchi, "Cutting-edge terahertz technology," *Nature photonics*, vol. 1, no. 2, pp. 97–105, 2007.

[2] D. N. Basov, R. D. Averitt, D. V. D. Marel, M. Dressel, and K. Haule, "Electrodynamics of correlated electron materials," *Reviews of Modern Physics*, vol. 83, pp. 471–541, 2011.

[3] T. Kampfrath, K. Tanaka, and K. A. Nelson, "Resonant and nonresonant control over matter and light by intense terahertz transients," *Nature Photonics*, vol. 7, no. 9, pp. 680–690, 2013.

[4] K. Reimann, "Table-top sources of ultrashort thz pulses," *Reports on Progress in Physics*, vol. 70, pp. 1597–1632, 2007.

[5] D. J. Cook and R. M. Hochstrasser, "Intense terahertz pulses by four-wave rectification in air," *Optics Letters*, vol. 25, p. 1210, 2000.

[6] J. Dai, X. Xie, and X. C. Zhang, "Terahertz wave amplification in gases with the excitation of femtosecond laser pulses," *Applied Physics Letters*, vol. 91, pp. 1–4, 2007.

[7] K.-Y. Kim, J. H. Glownia, A. J. Taylor, and G. Rodriguez, "Terahertz emission from ultrafast ionizing air in symmetry-broken laser fields," *Optics Express*, vol. 15, p. 4577, 2007.

[8] W. Hu, S. Kaiser, D. Nicoletti, C. R. Hunt, I. Gierz, M. C. Hoffmann, M. Le Tacon, T. Loew, B. Keimer, and A. Cavalleri, "Optically enhanced coherent transport in yba2cu3o6. 5 by ultrafast redistribution of interlayer coupling," *Nature materials*, vol. 13, no. 7, pp. 705–711, 2014.

[9] Y. Lan, B. J. Dringoli, D. A. Valverde-Chávez, C. S. Ponseca Jr, M. Sutton, Y. He, M. G. Kanatzidis, and D. G. Cooke, "Ultrafast correlated charge and lattice motion in a hybrid metal halide perovskite," *Science advances*, vol. 5, no. 5, p. eaaw5558, 2019.

[10] T. Oka and S. Kitamura, "Floquet engineering of quantum materials," *Annual Review of Condensed Matter Physics*, vol. 10, pp. 387–408, 2019.

[11] J. Zhang and R. D. Averitt, "Dynamics and control in complex transition metal oxides," *Annual Review of Materials Research*, vol. 44, pp. 19–43, 2014.

[12] A. S. Disa, T. F. Nova, and A. Cavalleri, "Engineering crystal structures with light," *Nature Physics*, vol. 17, 2021.

[13] S. Kamada, T. Yoshida, and T. Aoki, "The chirp-control of frequency-tunable narrowband terahertz pulses by nonlinearly chirped laser pulse beating," *Applied Physics Letters*, vol. 104, 2014.

[14] K. Uchida, H. Hirori, T. Aoki, C. Wolpert, T. Tamaya, K. Tanaka, T. Mochizuki, C. Kim, M. Yoshita, H. Akiyama, L. N. Pfeiffer, and K. W. West, "Time-resolved observation of coherent excitonic nonlinear response with a table-top narrowband thz pulse wave," *Applied Physics Letters*, vol. 107, 2015.

[15] S. W. Jolly, N. H. Matlis, F. Ahr, V. Leroux, T. Eichner, A.-L. Calendron, H. Ishizuki, T. Taira, F. X. Kärtner, and A. R. Maier, "Spectral phase control of interfering chirped pulses for high-energy narrowband terahertz generation," *Nature communications*, vol. 10, no. 1, pp. 1–8, 2019.

[16] B. Liu, H. Bromberger, A. Cartella, T. Gebert, M. Först, and A. Cavalleri, "Generation of narrowband, high-intensity, carrier-envelope phase-stable pulses tunable between 4 and 18 thz," *Optics letters*, vol. 42, no. 1, pp. 129–131, 2017.

[17] J. Das and M. Yamaguchi, "Tunable narrow band thz wave generation from laser induced gas plasma," *Optics Express*, vol. 18, p. 7038, 2010.

[18] C. Manzoni, M. Först, H. Ehrke, M. C. Hoffmann, and A. Cavalleri, "Single-shot detection and stabilization of carrier phase drifts of mid-ir pulses," in *International Conference on Ultrafast Phenomena*, p. TuE26, Optical Society of America, 2010.

[19] T. Yamakawa, N. Sono, T. Kitao, T. Morimoto, N. Kida, T. Miyamoto, and H. Okamoto, "Long-term stabilization of carrier envelope phases of mid-infrared pulses for the precise detection of phase-sensitive responses to electromagnetic waves," *AIP Advances*, vol. 10, no. 2, p. 025311, 2020.

[20] S. Liu, Z. Fan, C. Lu, J. Gui, C. Luo, S. Wang, Q. Liang, B. Zhou, A. Houard, A. Mysyrowicz, V. Kostin, and Y. Liu, "Coherent control of boosted terahertz radiation from air plasma pumped by a femtosecond three-color sawtooth field," *Physical Review A*, vol. 102, pp. 1–7, 2020.

[21] J.-M. Manceau, M. Massaouti, and S. Tzortzakis, "Coherent control of thz pulses polarization from femtosecond laser filaments in gases," *Optics Express*, vol. 18, p. 18894, 2010.

[22] J. Dai, N. Karpowicz, and X. C. Zhang, "Coherent polarization control of terahertz waves generated from two-color laser-induced gas plasma," *Physical Review Letters*, vol. 103, pp. 1–4, 2009.

[23] Z. Zhang, Y. Chen, S. Cui, F. He, M. Chen, Z. Zhang, J. Yu, L. Chen, Z. Sheng, and J. Zhang, "Manipulation of polarizations for broadband terahertz waves emitted from laser plasma filaments," *Nature Photonics*, vol. 12, no. 9, pp. 554–559, 2018.

[24] H. Wen and A. M. Lindenberg, "Coherent terahertz polarization control through manipulation of electron trajectories," *Phys. Rev. Lett.*, vol. 103, p. 023902, Jul 2009.

[25] G. Yumoto, R. Matsunaga, H. Hibino, and R. Shimano, "Ultrafast terahertz nonlinear optics of landau level transitions in a monolayer graphene," *Physical Review Letters*, vol. 120, no. 10, p. 107401, 2018.

[26] J. W. McIver, B. Schulte, F.-U. Stein, T. Matsuyama, G. Jotzu, G. Meier, and A. Cavalleri, "Light-induced anomalous hall effect in graphene," *Nature physics*, vol. 16, no. 1, pp. 38–41, 2020.

[27] Z. Chen, X. Zhou, C. A. Werley, and K. A. Nelson, "Generation of high power tunable multicycle teraherz pulses," *Applied Physics Letters*, vol. 99, pp. 1–4, 2011.

[28] A. S. Weling, B. B. Hu, N. M. Froberg, and D. H. Auston, "Generation of tunable narrowband thz radiation from large aperture photoconducting antennas," *Applied Physics Letters*, vol. 64, pp. 137–139, 1994.

[29] P. Ungelenk, M. Höner, H. Huck, S. Khan, C. Mai, A. M. A. D. Heide, C. Evain, C. Szwaj, and S. Bielawski, "Continuously tunable narrowband pulses in the thz gap from laser-modulated electron bunches in a storage ring," *Physical Review Accelerators and Beams*, vol. 20, pp. 1–12, 2017.

[30] S. Bielawski, C. Evain, T. Hara, M. Hosaka, M. Katoh, S. Kimura, A. Mochihashi, M. Shimada, C. Szwaj, T. Takahashi, and Y. Takashima, "Tunable narrowband terahertz emission from mastered laser-electron beam-interaction," *Nature Physics*, vol. 4, pp. 390–393, 2008.

[31] A. S. Weling and D. H. Auston, "Terahertz radiation in free space," *America*, vol. 13, pp. 2783–2791, 1996.

[32] K. Y. Kim, "Generation of coherent terahertz radiation in ultrafast laser-gas interactions," *Physics of Plasmas*, vol. 16, 2009.

[33] M. V. Ammosov, N. B. Delone, and V. P. Krainov, "Tunnel ionization of complex atoms and of atomic ions in an alternating electromagnetic field," *Zh. Eksp. Teor. Fiz.*, vol. 91, pp. 2008–2013, 1986.
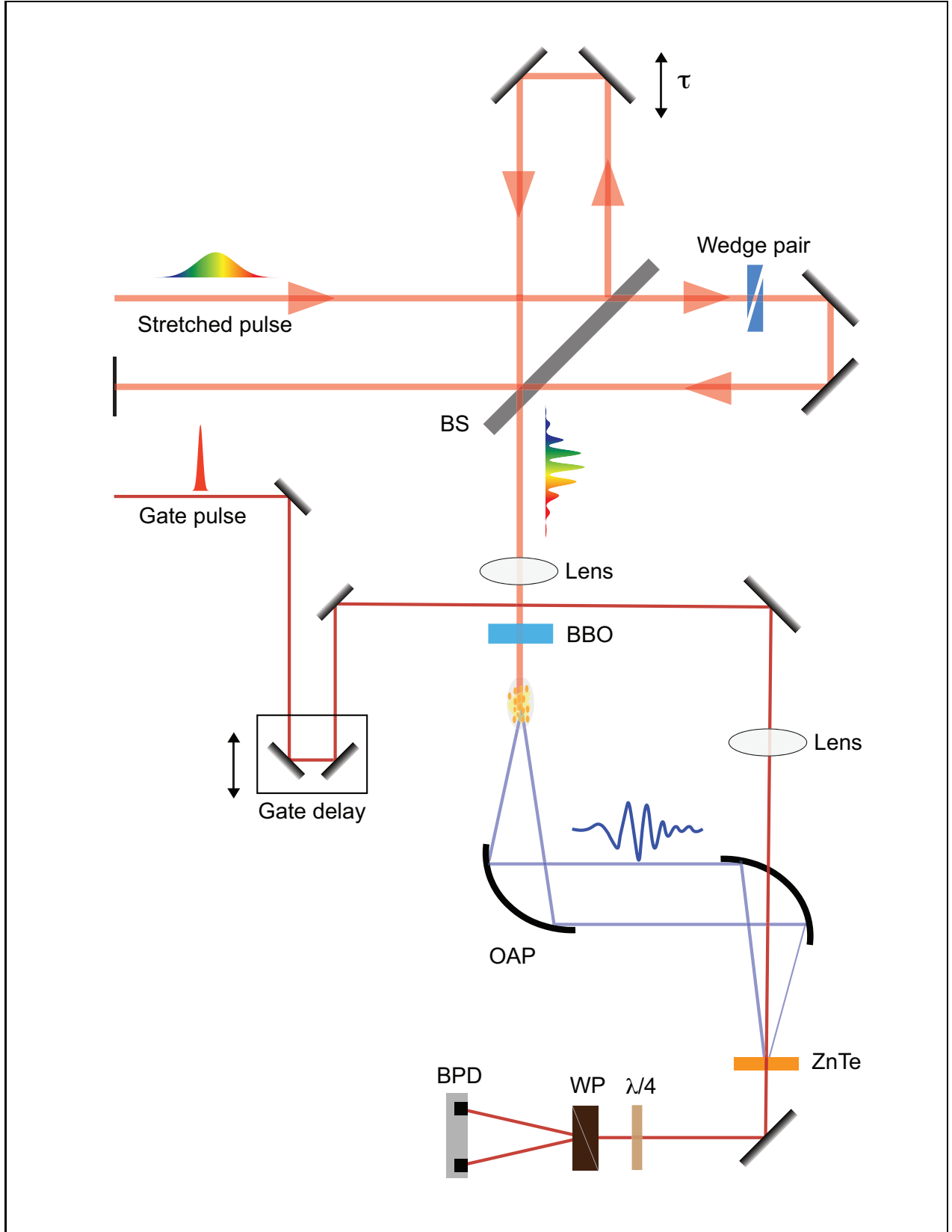
FIG. 1. The schematic diagram of the experiment setup. BS: non-polarized beam splitter, OAP: off-axis parabolic mirror, WP: Wollaston prism, BPD: Balanced Photodetector
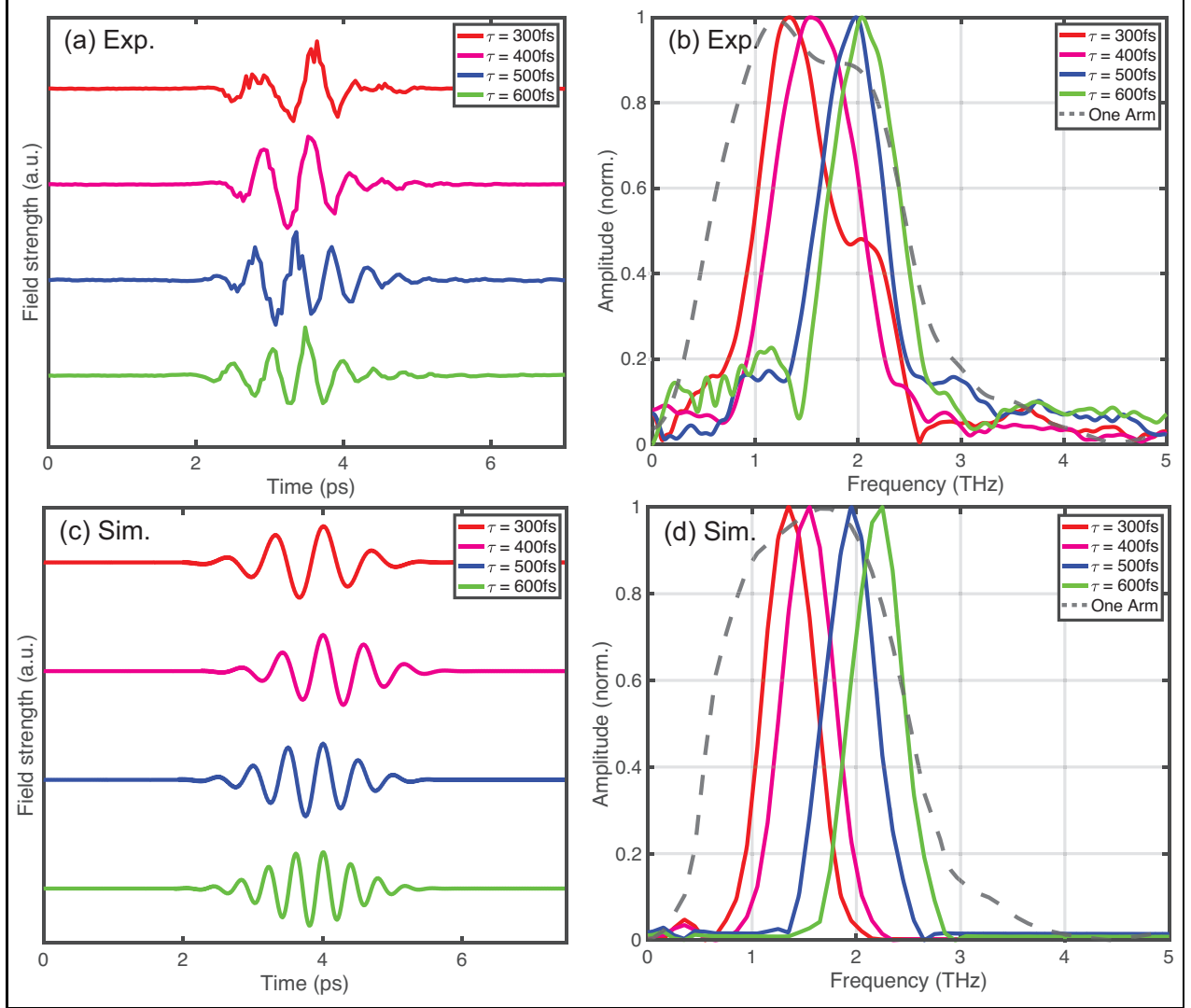
FIG. 2. (a) Time-domain signal of the THz radiation at four representative delays τ obtained from the experiment. (b) The corresponding intensity spectrum obtained after Fourier transform. The dashed line represents the spectrum obtained from one single arm using ZnTe as the EO-sampling crystal, from which a narrow-band characteristic is absent. (c) Time-domain signal of the THz radiation for four different values of delay τ obtained from the numerical simulation. (d) The corresponding intensity spectrum from simulation. The dashed line represents the calculated single-arm spectrum.
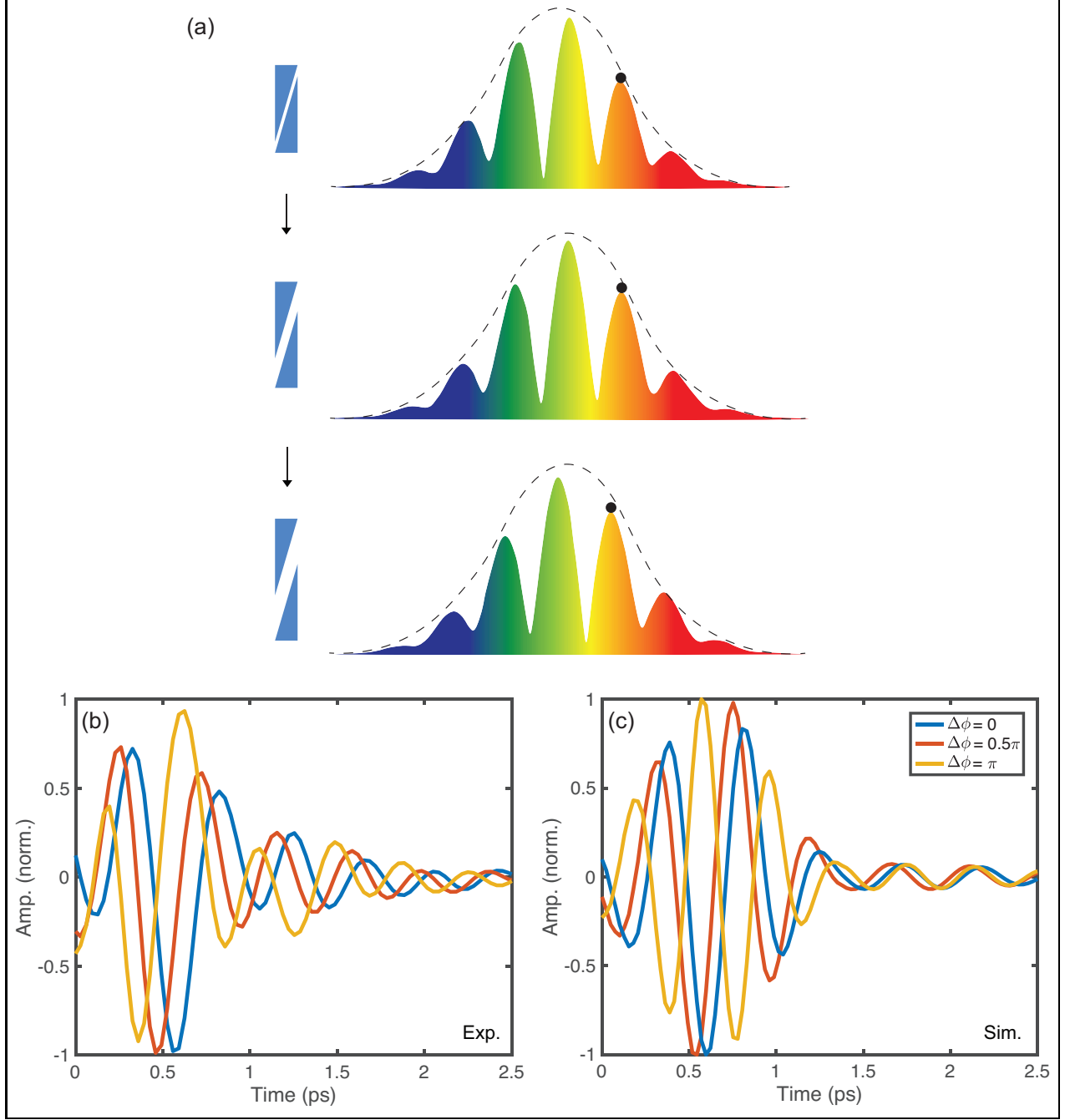
FIG. 3. (a) The scheme diagram showing the functionality of the wedge pair on the phase modulation of pulse sequence. The black dot in the figure represents a fixed point in time. (b) Experimental result of the time-domain signal of the THz radiation for three different values of displacement Δx of the wedge pair, a CEP shift of approximate value of π can be observed from the blue to yellow curve. (c) The numerical simulation result for phase $\Delta\phi = 0, \pi/2$ and π.